SLADe (Quad) Project

Control and Simulation Report

13 February 2009

Iain K. Peddle

Introduction

This document begins by providing the details of the mathematical model developed to describe the motion of the SLADe quad-rotor aircraft through space. The model is then linearised about a hover flight trim condition and five linear, decoupled control systems are designed using a successive loop closure approach. The control system allows the aircraft to navigate in three dimensional space while maintaining an arbitrary heading angle. It is also possible to update the heading angle on the fly without affecting the translational motion of the aircraft. During the controller design it is assumed that the full state vector is available for feedback. A kinematic state estimator is used to provide the full state vector for feedback. The estimator makes use of MEMS angular rate gyroscopes and accelerometers, a 3-axis magnetometer and a GPS receiver. The feasibility of using these sensors in an operational environment is also discussed. The Simulink block diagram used to simulate the aircraft, controller and estimator is then described. Effects such as sensor noise and wind are included in the simulator for increased fidelity. Results from applicable simulation runs under typical disturbance conditions show that the control system performs adequately at low to medium speed flight.

Complete nonlinear model for near hover flight

The six degree of freedom equations of motion for a rigid body are,

$$
\begin{aligned}
X &= m(\dot{U} + WQ - VR) \\
Y &= m(\dot{V} + UR - WP) \\
Z &= m(\dot{W} + VP - UQ)
\end{aligned}
$$

$$
\begin{aligned}
L &= I_x\dot{P} + QR(I_z - I_y) \\
M &= I_y\dot{Q} + PR(I_x - I_z) \\
N &= I_z\dot{R} + PQ(I_y - I_x)
\end{aligned}
$$

$$
\begin{bmatrix} \dot{\Phi} \\ \dot{\Theta} \\ \dot{\Psi} \end{bmatrix} = \begin{bmatrix} 1 & \sin\Phi\tan\Theta & \cos\Phi\tan\Theta \\ 0 & \cos\Phi & -\sin\Phi \\ 0 & \sin\Phi\sec\Theta & \cos\Phi\sec\Theta \end{bmatrix} \begin{bmatrix} P \\ Q \\ R \end{bmatrix} \qquad |\Theta| \neq \frac{\pi}{2}
$$

$$
\begin{bmatrix} \dot{N} \\ \dot{E} \\ \dot{D} \end{bmatrix} = \begin{bmatrix} C_\Psi C_\Theta & C_\Psi S_\Theta S_\Phi - S_\Psi C_\Phi & C_\Psi S_\Theta C_\Phi + S_\Psi S_\Phi \\ S_\Psi C_\Theta & S_\Psi S_\Theta S_\Phi + C_\Psi C_\Phi & S_\Psi S_\Theta C_\Phi - C_\Psi S_\Phi \\ -S_\Theta & C_\Theta S_\Phi & C_\Theta C_\Phi \end{bmatrix} \begin{bmatrix} U \\ V \\ W \end{bmatrix} \qquad C_{(\,)} = \cos(\,),\ S_{(\,)} = \sin(\,)
$$

where the notation used is standard [1]. Euler angles have been employed to parameterise the attitude due to their simplicity and due to the fact that the aircraft's pitch angle will remain far from positive and negative ninety degrees. The forces acting on the aircraft are considered to arise from,

- Aerodynamic lift and drag due to rotor motion
- Gravity
- Aerodynamic lift and drag due the motion of the body relative to the wind

Mathematically, these forces and their corresponding moments are modelled as follows,

$$
\begin{aligned}
X &= -mg\sin\Theta - D_X \\
Y &= mg\cos\Theta\sin\Phi - D_Y \\
Z &= -(T_1 + T_2 + T_3 + T_4) - L + mg\cos\Theta\cos\Phi \\
L &= d\left(T_4 - T_2\right) \\
M &= d\left(T_1 - T_3\right) \\
N &= r_D\left(-T_1 + T_2 - T_3 + T_4\right)/R_{LD}
\end{aligned}
$$

with,

$$\begin{bmatrix} D_X \\ D_Y \end{bmatrix} = \begin{bmatrix} \cos\Psi & \sin\Psi \\ -\sin\Psi & \cos\Psi \end{bmatrix} \begin{bmatrix} \cos\Psi_{BW} \\ \sin\Psi_{BW} \end{bmatrix} \bar{D}$$

$$\bar{D} = \frac{1}{2}\rho \bar{V}_{BW}^2 A_D C_D$$

$$\bar{V}_{BW} = \sqrt{\left(\dot{N}^{BI} - \dot{N}^{WI}\right)^2 + \left(\dot{E}^{BI} - \dot{E}^{WI}\right)^2}$$

$$\Psi_{BW} = \tan^{-1}\left(\frac{\dot{E}^{BI} - \dot{E}^{WI}}{\dot{N}^{BI} - \dot{N}^{WI}}\right)$$

with rotor lag dynamics,

$$\begin{aligned} \dot{T}_1 &= \left(-T_1 + T_{1_R}\right)/\tau \\ \dot{T}_2 &= \left(-T_2 + T_{2_R}\right)/\tau \\ \dot{T}_3 &= \left(-T_3 + T_{3_R}\right)/\tau \\ \dot{T}_4 &= \left(-T_4 + T_{4_R}\right)/\tau \end{aligned}$$

The lift and drag variables in the force equations are stub parameters at this point. These will be expanded upon for higher speed flight. The parameters used in the model are described in Appendix A. Now define virtual actuators (states actually when the lag dynamics are considered) to simplify the model,

$$\begin{aligned} \delta_T &= T_1 + T_2 + T_3 + T_4 \\ \delta_A &= T_4 - T_2 \\ \delta_E &= T_1 - T_3 \\ \delta_R &= -T_1 + T_2 - T_3 + T_4 \end{aligned}$$

By differentiating each equation with respect to time and substituting from above it is straightforward to show that,

$$\begin{aligned} \dot{\delta}_T &= \left(-\delta_T + \delta_{T_R}\right)/\tau \\ \dot{\delta}_A &= \left(-\delta_A + \delta_{A_R}\right)/\tau \\ \dot{\delta}_E &= \left(-\delta_E + \delta_{E_R}\right)/\tau \\ \dot{\delta}_R &= \left(-\delta_R + \delta_{R_R}\right)/\tau \end{aligned}$$

where,

$$\begin{aligned} \delta_{T_R} &= T_{1_R} + T_{2_R} + T_{3_R} + T_{4_R} \\ \delta_{A_R} &= T_{4_R} - T_{2_R} \\ \delta_{E_R} &= T_{1_R} - T_{3_R} \\ \delta_{R_R} &= -T_{1_R} + T_{2_R} - T_{3_R} + T_{4_R} \end{aligned}$$

Thus it is seen that if the thrust lag dynamics are linear as modelled, then the virtual actuator dynamics are linear too. If these dynamics are not linear, then dynamic inversion techniques could be applied to enforce the linearity. Substituting the virtual actuator definitions into the dynamics changes the force and moment equations to,

$$X = -mg\sin\Theta - D_X$$
$$Y = mg\cos\Theta\sin\Phi - D_Y$$
$$Z = -\delta_T - L + mg\cos\Theta\cos\Phi$$
$$L = d\delta_A$$
$$M = d\delta_E$$
$$N = r_D\delta_R / R_{LD}$$

with the virtual actuator lag dynamics provided above. For control purposes we need to be able to convert the virtual control inputs defined back to individual thrust commands. Thus, we seek the 4 by 4 mixing matrix that relates virtual control inputs back to individual thrust commands. Beginning with the definition of the virtual control inputs above we can write,

$$\begin{bmatrix} \delta_{T_R} \\ \delta_{A_R} \\ \delta_{E_R} \\ \delta_{R_R} \end{bmatrix} = \begin{bmatrix} 1 & 1 & 1 & 1 \\ 0 & -1 & 0 & 1 \\ 1 & 0 & -1 & 0 \\ -1 & 1 & -1 & 1 \end{bmatrix} \begin{bmatrix} T_{1_R} \\ T_{2_R} \\ T_{3_R} \\ T_{4_R} \end{bmatrix}$$

We find the mixing matrix by taking the inverse of the above matrix,

$$\begin{bmatrix} T_{1_R} \\ T_{2_R} \\ T_{3_R} \\ T_{4_R} \end{bmatrix} = \begin{bmatrix} 0.25 & 0 & 0.5 & -0.25 \\ 0.25 & -0.5 & 0 & 0.25 \\ 0.25 & 0 & -0.5 & -0.25 \\ 0.25 & 0.5 & 0 & 0.25 \end{bmatrix} \begin{bmatrix} \delta_{T_R} \\ \delta_{A_R} \\ \delta_{E_R} \\ \delta_{R_R} \end{bmatrix}$$

Linearising the model about a hover trim condition

Define the hover trim condition,

$$U_0 = V_0 = W_0 = 0$$
$$P_0 = Q_0 = R_0 = 0$$
$$\Phi_0 = \Theta_0 = 0$$

Note that Ψ, N, E and D do not form part of the trim condition and will be maintained as complete variables in the analysis to follow. Writing the motion variables that define the trim condition as the sum of a trim condition value and a small perturbation, the equations of motion can be written as follows,

$$x = m\dot{u} \qquad y = m\dot{v} \qquad z = m\dot{w}$$
$$l = I_x\dot{p} \qquad m = I_y\dot{q} \qquad n = I_z\dot{r}$$
$$\dot{\phi} = p \qquad \dot{\theta} = q \qquad \dot{\Psi} = r$$
$$\dot{N} = u\cos\Psi_0 - v\sin\Psi_0 \qquad \dot{E} = u\sin\Psi_0 + v\cos\Psi_0 \qquad \dot{D} = w$$

where, by analysing the equations at the trim condition it can be shown that,

$$X_0 = Y_0 = Z_0 = 0 \qquad L_0 = M_0 = N_0 = 0$$

Applying small perturbation theory to the force and moment equations and ignoring the lift and drag stubs for now gives,

$$x = -mg\theta$$
$$y = mg\phi$$

$$z = -\delta_T + mg$$
$$l = d\delta_A$$
$$m = d\delta_E$$
$$n = r_D\delta_R / R_{LD}$$

with the already linear actuator dynamics,

$$\dot{\delta}_T = \left(-\delta_T + \delta_{T_R}\right)\Big/\tau$$
$$\dot{\delta}_A = \left(-\delta_A + \delta_{A_R}\right)\Big/\tau$$
$$\dot{\delta}_E = \left(-\delta_E + \delta_{E_R}\right)\Big/\tau$$
$$\dot{\delta}_R = \left(-\delta_R + \delta_{R_R}\right)\Big/\tau$$

Note that the virtual actuators have been left as full variables for convenience. The only effect this has is to introduce the gravity bias into the vertical velocity dynamics since the roll, pitch and yaw virtual actuators are all centred about zero. Bringing the linearised force and moment model together with the linearised kinematic equations and writing in state space form, the four decoupled linear systems are found,

Longitudinal:
$$\begin{bmatrix}\dot{\delta}_E\\ \dot{q}\\ \dot{\theta}\\ \dot{u}\end{bmatrix} = \begin{bmatrix}-1/\tau & 0 & 0 & 0\\ d/I_y & 0 & 0 & 0\\ 0 & 1 & 0 & 0\\ 0 & 0 & -g & 0\end{bmatrix}\begin{bmatrix}\delta_E\\ q\\ \theta\\ u\end{bmatrix} + \begin{bmatrix}1/\tau\\ 0\\ 0\\ 0\end{bmatrix}\delta_{E_R}$$

Lateral:
$$\begin{bmatrix}\dot{\delta}_A\\ \dot{p}\\ \dot{\phi}\\ \dot{v}\end{bmatrix} = \begin{bmatrix}-1/\tau & 0 & 0 & 0\\ d/I_x & 0 & 0 & 0\\ 0 & 1 & 0 & 0\\ 0 & 0 & g & 0\end{bmatrix}\begin{bmatrix}\delta_A\\ p\\ \phi\\ v\end{bmatrix} + \begin{bmatrix}1/\tau\\ 0\\ 0\\ 0\end{bmatrix}\delta_{A_R}$$

Directional:
$$\begin{bmatrix}\dot{\delta}_R\\ \dot{r}\\ \dot{\Psi}\end{bmatrix} = \begin{bmatrix}-1/\tau & 0 & 0\\ r_D/\left(R_{LD}I_z\right) & 0 & 0\\ 0 & 1 & 0\end{bmatrix}\begin{bmatrix}\delta_R\\ r\\ \Psi\end{bmatrix} + \begin{bmatrix}1/\tau\\ 0\\ 0\end{bmatrix}\delta_{R_R}$$

Heave:
$$\begin{bmatrix}\dot{\delta}_T\\ \dot{w}\\ \dot{D}\end{bmatrix} = \begin{bmatrix}-1/\tau & 0 & 0\\ -1/m & 0 & 0\\ 0 & 1 & 0\end{bmatrix}\begin{bmatrix}\delta_T\\ w\\ D\end{bmatrix} + \begin{bmatrix}1/\tau\\ 0\\ 0\end{bmatrix}\delta_{T_R} + \begin{bmatrix}0\\ g\\ 0\end{bmatrix}$$

with the nonlinear navigation dynamics,

Navigation:
$$\begin{bmatrix}\dot{N}\\ \dot{E}\end{bmatrix} = \begin{bmatrix}\cos\Psi & -\sin\Psi\\ \sin\Psi & \cos\Psi\end{bmatrix}\begin{bmatrix}u\\ v\end{bmatrix}$$

Control system design

For control system design purposes it will be assumed that the full state vector is available for feedback. This assumption will be realised in the next section where the architecture of a full state estimator is described. A successive loop closure control strategy is adopted instead of a full state feedback approach. Successive loop closure is a far more practical and intuitive approach than full state feedback and tends to render robust, easy to use control systems. It also eases the practical testing process by allowing successive loops to be armed, thus enabling a human pilot to fly the aircraft in a stability augmentation mode. This is essential for the quad-rotor configuration.

The controller design is presented in symbolic form below. Only the controller structure and the arguments promoting that structure are presented here. The final values for the feedback gains specific to SLADe are listed in Appendix B.

Longitudinal control system

The longitudinal dynamics are restated below for convenience,

$$\begin{bmatrix} \dot{\delta}_E \\ \dot{q} \\ \dot{\theta} \\ \dot{u} \end{bmatrix} = \begin{bmatrix} -1/\tau & 0 & 0 & 0 \\ d/I_y & 0 & 0 & 0 \\ 0 & 1 & 0 & 0 \\ 0 & 0 & -g & 0 \end{bmatrix} \begin{bmatrix} \delta_E \\ q \\ \theta \\ u \end{bmatrix} + \begin{bmatrix} 1/\tau \\ 0 \\ 0 \\ 0 \end{bmatrix} \delta_{E_R}$$

We begin with pitch rate feedback to improve the aircraft's pitch damping and to quickly negate the adverse effects of disturbance torques. From a control system design perspective it is best to counter any disturbances as quickly as possible using the inner most control loops as these typically directly command restoring forces and moments. Thus, to counter the effect of disturbance torques due to factors such as misalignment of the rotors, offsets in the centre of gravity position and constant winds, we chose to design a Proportional-Integral (PI) type controller. However, the proportional part will be designed to carry out most of the damping, while a slow integrator will be used to counter disturbances in the steady state. Thus, the following control law is employed,

$$\delta_{E_R} = K_{q_P}\left(q_R - q\right) + K_{q_I}\int_t \left(q_R - q\right) dt$$

With the pitch damping controller in place we now design a pitch angle controller. The effects of steady state disturbances due to the factors listed previously will already have be removed by the inner pitch rate control system. Thus, there is no need to have an integrator in the compensator here. However, if the pitch rate sensor/estimate displays a bias then there will be a steady state error between commanded and actual pitch angle if no compensator integrator is added. If the proportional gain is made high enough and the pitch rate bias is small, then the offset will be negligible. This is most often the case and it will be shown by simulation that the error induced by this effect does not warrant the complications caused by the addition of a compensator integrator. Thus, we simply design a proportional feedback controller of the form,

$$q_R = K_\theta\left(\theta_R - \theta\right)$$

Note that the pitch angle controller drives the reference of the pitch rate controller. The next controller designed is a longitudinal velocity controller. Unlike with the original ducted fan SLADe, there is no longer a right half plane zero constraining the bandwidth of this system. With steady state disturbances rejected by the inner control loops, a proportional controller is again employed to stabilise the longitudinal velocity dynamics,

$$\theta_R = K_u\left(u_R - u\right)$$

where the longitudinal velocity controller drives the pitch angle controller. This controller can be upgraded to an PI type controller at a later stage if necessary to provide rejection of constant forces on the system e.g. drag during high speed forward flight. At this point, we are able to control the velocity along the axial unit vector of the aircraft. In the section on navigation control, we will look at using the axial velocity reference input to regulate the navigation error to zero.

Lateral control system

The lateral dynamics are restated below for convenience,

$$\begin{bmatrix} \dot{\delta}_A \\ \dot{p} \\ \dot{\phi} \\ \dot{v} \end{bmatrix} = \begin{bmatrix} -1/\tau & 0 & 0 & 0 \\ d/I_x & 0 & 0 & 0 \\ 0 & 1 & 0 & 0 \\ 0 & 0 & g & 0 \end{bmatrix} \begin{bmatrix} \delta_A \\ p \\ \phi \\ v \end{bmatrix} + \begin{bmatrix} 1/\tau \\ 0 \\ 0 \\ 0 \end{bmatrix} \delta_{A_R}$$

Due to the symmetry of the aircraft, the lateral control system is of exactly the same form as the longitudinal control system. The controller is summarised as follows. A PI roll rate controller is employed,

$$\delta_{A_R} = K_{p_P}\left(p_R - p\right) + K_{p_I}\int_t \left(p_R - p\right)dt$$

A proportional roll angle controller drives the roll rate reference input,

$$p_R = K_\phi\left(\phi_R - \phi\right)$$

A proportional lateral velocity controller drives the roll angle reference input,

$$\phi_R = K_v\left(v_R - v\right)$$

Directional control system

The directional dynamics are restated below for convenience,

$$\begin{bmatrix}\dot{\delta}_R\\ \dot{r}\\ \dot{\Psi}\end{bmatrix} = \begin{bmatrix}-1/\tau & 0 & 0\\ r_D/\left(R_{LD}I_z\right) & 0 & 0\\ 0 & 1 & 0\end{bmatrix}\begin{bmatrix}\delta_R\\ r\\ \Psi\end{bmatrix} + \begin{bmatrix}1/\tau\\ 0\\ 0\end{bmatrix}\delta_{R_R}$$

A PI yaw rate controller strategy is adopted for similar reasons to those stated in the longitudinal and lateral controllers. Thus,

$$\delta_{R_R} = K_{r_P}\left(r_R - r\right) + K_{r_I}\int_t \left(r_R - r\right)dt$$

A proportional feedback yaw angle controller is now designed. Note that the yaw angle referred to in the dynamics is the absolute angle and not a small perturbation. Thus, this controller allows us to command the absolute angle. The control law is,

$$r_R = K_\Psi\left(\Psi_R - \Psi\right)$$

Heave control system

The heave dynamics are,

$$\begin{bmatrix}\dot{\delta}_T\\ \dot{w}\\ \dot{D}\end{bmatrix} = \begin{bmatrix}-1/\tau & 0 & 0\\ -1/m & 0 & 0\\ 0 & 1 & 0\end{bmatrix}\begin{bmatrix}\delta_T\\ w\\ D\end{bmatrix} + \begin{bmatrix}1/\tau\\ 0\\ 0\end{bmatrix}\delta_{T_R} + \begin{bmatrix}0\\ g\\ 0\end{bmatrix}$$

Again a successive loop closure approach is adopted. First, the vertical climb rate is fed back using a PI controller to provide damping of the heave dynamics and negate any steady state disturbances introduced by inaccuracies in the thrust model and the aircraft mass. The control law is thus,

$$\delta_{T_R} = K_{w_P}\left(w_R - w\right) + K_{w_I}\int_t \left(w_R - w\right)dt$$

Finally, a proportional feedback altitude controller is implemented. The controller drives the climb rate input. Note that similarly to the heading angle variable above, the altitude variable is also an absolute value and not a small perturbation. Thus the controller below allows us to command the absolute altitude.

$$w_R = K_D\left(D_R - D\right)$$

Navigation control system

The navigation dynamics are restated below for convenience,

$$\begin{bmatrix}\dot{N}\\ \dot{E}\end{bmatrix} = \begin{bmatrix}\cos\Psi & -\sin\Psi\\ \sin\Psi & \cos\Psi\end{bmatrix}\begin{bmatrix}u\\ v\end{bmatrix}$$

At this stage, among others, controllers for the longitudinal velocity, lateral velocity and absolute heading angle have been designed. Thus, with reference to the above equation, the rate of change of North-East position is over controlled, with three control inputs regulating two position outputs. However, it is desired to be able to regulate the heading angle arbitrarily during North-East translation, effectively removing this variable as a control input to the navigation dynamics. The navigation controller should thus be able to regulate the position error to zero over time, without regard for the heading angle. Given the desired North-East positions of the vehicle, N_R and E_R respectively, the North-East position error is defined as follows,

$$\begin{bmatrix}N_E\\ E_E\end{bmatrix} = \begin{bmatrix}N_R\\ E_R\end{bmatrix} - \begin{bmatrix}N\\ E\end{bmatrix}$$

The navigation error coordinates can be instantaneously converted to body axis coordinates using the transformation,

$$\begin{bmatrix}X_E\\ Y_E\end{bmatrix} = \begin{bmatrix}\cos\Psi & \sin\Psi\\ -\sin\Psi & \cos\Psi\end{bmatrix}\begin{bmatrix}N_E\\ E_E\end{bmatrix}$$

The dynamics of the navigation error coordinates in body axes are,

$$\begin{aligned}\begin{bmatrix}\dot{X}_E\\ \dot{Y}_E\end{bmatrix} &= \begin{bmatrix}\cos\Psi & \sin\Psi\\ -\sin\Psi & \cos\Psi\end{bmatrix}\begin{bmatrix}\dot{N}_E\\ \dot{E}_E\end{bmatrix} - \dot{\Psi}\begin{bmatrix}\sin\Psi & -\cos\Psi\\ \cos\Psi & \sin\Psi\end{bmatrix}\begin{bmatrix}N_E\\ E_E\end{bmatrix}\\ &= \begin{bmatrix}\cos\Psi & \sin\Psi\\ -\sin\Psi & \cos\Psi\end{bmatrix}\begin{bmatrix}\dot{N}_E\\ \dot{E}_E\end{bmatrix} + r\begin{bmatrix}Y_E\\ -X_E\end{bmatrix}\end{aligned}$$

Assuming that a constant reference position is commanded, the navigation error dynamics are,

$$\begin{bmatrix}\dot{N}_E\\ \dot{E}_E\end{bmatrix} = -\begin{bmatrix}\cos\Psi & -\sin\Psi\\ \sin\Psi & \cos\Psi\end{bmatrix}\begin{bmatrix}u\\ v\end{bmatrix}$$

Substituting the above error dynamics into the navigation error dynamics in body coordinates gives,

$$\begin{aligned}\begin{bmatrix}\dot{X}_E\\ \dot{Y}_E\end{bmatrix} &= -\begin{bmatrix}\cos\Psi & \sin\Psi\\ -\sin\Psi & \cos\Psi\end{bmatrix}\begin{bmatrix}\cos\Psi & -\sin\Psi\\ \sin\Psi & \cos\Psi\end{bmatrix}\begin{bmatrix}u\\ v\end{bmatrix} + r\begin{bmatrix}Y_E\\ -X_E\end{bmatrix}\\ &= -\begin{bmatrix}u\\ v\end{bmatrix} + r\begin{bmatrix}Y_E\\ -X_E\end{bmatrix}\end{aligned}$$

Assuming that the yaw rate remains low during translational motion, we can ignore the second cross coupling term in the equation above. This condition can be enforced by setting the saturation limit on yaw rate in the directional controller appropriately. Thus, the navigation error dynamics simply reduce to the linear decoupled dynamics,

$$\begin{bmatrix} \dot{X}_E \\ \dot{Y}_E \end{bmatrix} = -\begin{bmatrix} u \\ v \end{bmatrix}$$

A proportional control law is designed to drive the navigation error coordinates in body axes to zero over time. Note that the longitudinal and lateral dynamics are also included in the design of the controller. The control law is summarised below,

$$\begin{bmatrix} u \\ v \end{bmatrix} = \begin{bmatrix} K_N & 0 \\ 0 & K_E \end{bmatrix} \begin{bmatrix} X_E \\ Y_E \end{bmatrix}$$

which can be written in terms of the inertial coordinates as follows,

$$\begin{bmatrix} u \\ v \end{bmatrix} = \begin{bmatrix} K_N & 0 \\ 0 & K_E \end{bmatrix} \begin{bmatrix} \cos\Psi & \sin\Psi \\ -\sin\Psi & \cos\Psi \end{bmatrix} \begin{bmatrix} N_R - N \\ E_R - E \end{bmatrix}$$

Due to the symmetry of the vehicle, the feedback gains K_N and K_E will be identical.

Summary of the controllers

A summary of the control system is provided below,

Longitudinal:
$$\delta_{E_R} = K_{q_P}(q_R - q) + K_{q_I}\int_t (q_R - q)\,dt$$
$$q_R = K_\theta(\theta_R - \theta)$$
$$\theta_R = K_u(u_R - u)$$

Lateral:
$$\delta_A = K_{p_P}(p_R - p) + K_{p_I}\int_t (p_R - p)\,dt$$
$$p_R = K_\phi(\phi_R - \phi)$$
$$\phi_R = K_v(v_R - v)$$

Directional:
$$\delta_{R_R} = K_{r_P}(r_R - r) + K_{r_I}\int_t (r_R - r)\,dt$$
$$r_R = K_r(\Psi_R - \Psi)$$

Heave:
$$\delta_{T_R} = K_{w_P}(w_R - w) + K_{w_I}\int_t (w_R - w)\,dt$$
$$w_R = K_D(D_R - D)$$

Navigation:
$$\begin{bmatrix} u \\ v \end{bmatrix} = \begin{bmatrix} K_N & 0 \\ 0 & K_E \end{bmatrix} \begin{bmatrix} \cos\Psi & \sin\Psi \\ -\sin\Psi & \cos\Psi \end{bmatrix} \begin{bmatrix} N_R - N \\ E_R - E \end{bmatrix}$$

When the controllers are practically implemented, integrator anti-windup algorithms will be used to protect the compensator integrators from building up in the event of actuator saturation. Signal saturation blocks will also be placed at the reference inputs of each successive loop to ensure that the closed loop system enters a constant slew rate mode when reference inputs exceed a certain limit. Rate limiters on the reference inputs provided by an operator will also ensure that large control inputs are not instantaneously commanded for step like inputs.

With the longitudinal, lateral, directional, heave and navigation controllers in place, it is possible to regulate the three dimensional position of the aircraft at an arbitrary heading angle. Of course, by manually providing references for inner loop controllers, the aircraft can be operated in different modes e.g. velocity control mode or rate control mode for piloted flight.

State estimation

State estimation will not be addressed in detail in this report since a standard, vehicle independent kinematic state estimator is readily available at SU. This estimator has been implemented and tested on a number of fixed and rotary wing UAVs and as such presents little risk to the project. The paragraphs below however will address the sensors used in the estimator, their reliability and their applicability to the operational environment.

The estimator makes use of angular rate gyroscopes, accelerometers, a GPS receiver and a magnetometer. The gyroscopes are used to propagate the attitude of the aircraft, which in turn is bounded by updates from the GPS receiver, the magnetometer and the accelerometers. In homogonous, well behaved operational environments, acceptable (in terms of ths specifications for this project) state accuracy can be obtained by using only low costs sensors, e.g. MEMS inertial sensors, low cost GPS and low cost magnetometer. As the severity of the operational environment is increased, the weak link in the estimator is revealed to be the magnetometer. This sensor is difficult to calibrate and is very sensitive to 'noise' sources e.g. varying currents flowing to the electric motors and changing hard iron effects when near to and far from the boat. Because the magnetometer is used to update attitude in the estimator, the performance of the estimator can severely degrade if noise or biases are induced on the magnetometer.

The current estimator architecture does allow for the dependency of the roll and pitch attitude on the magnetometer to be removed with negligible degradation in accuracy. Only the heading angle then remains dependent on the magnetometer measurements, requiring this signal to bound the heading propagation error. Given the importance of accurate heading regulation in this project, it may be desirable to remove this final magnetometer dependency too. Without the magnetometer, the sensor pack would be very robust in the sense that none of the sensors would be strongly dependent, for calibration or operation, on the operational environment.

Considering the options then, all standard off-the-shelf MEMS based Attitude and Heading Reference Systems (AHRS) such as the Crossbow AHRS440 make use of a magnetometer to bound attitude. Although these devices claim to provide promising results even under high dynamic conditions, their internal magnetometer will still remain susceptible to the effects discussed above, thus making them undesirable for a robust solution. Given the very limited flight time of SLADe, one very feasible and still affordable option would be to replace just the MEMS yaw rate gyroscope with a Fibre Optic Gyroscope (FOG). FOG technology would allow the yaw rate gyroscope to be propagated without update with better than sub degree accuracy at the end of a typical mission. Although a magnetometer will still be used during the advanced concept demonstrator phase of the project, consideration of the FOG option is recommended for the final system design.

Simulation and evaluation

The aircraft model, control system and state estimator were created in MATLAB's Simulink environment for full simulation purposes. Figure 1 below shows the highest level of the block diagram simulator.

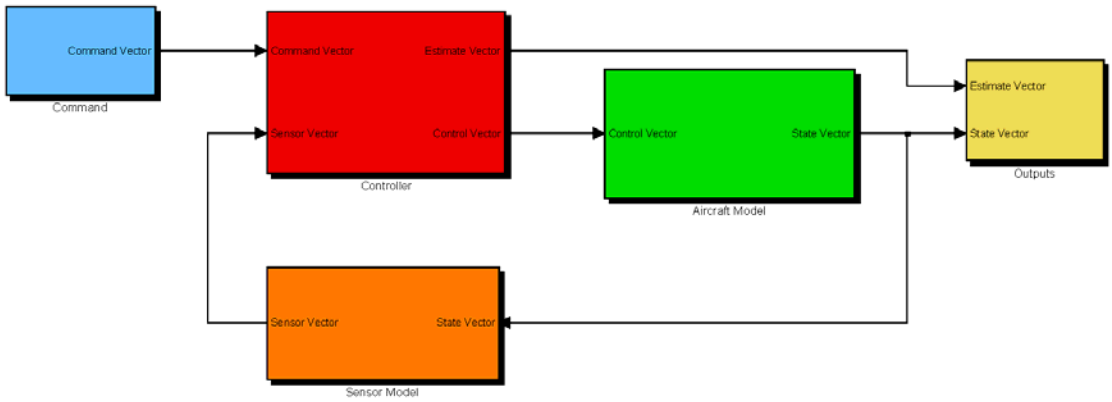

Figure 1 – Highest Level of Simulink Block Diagram

The simulator was used to evaluate the performance of a basic first generation, hover and low speed flight control system based in the original SLADe (Ducted Fan) design. The simulation results shown below were carried out with the feedback gains as stated in Appendix B. The simulation commanded the vehicle to execute the following sequence of events,

- The aircraft starts at the origin of the North-East axis system with an altitude of 10m a heading of 0 degrees.
- After 5s, the aircraft is commanded to fly 100m East.
- After 40s, the aircraft's heading is commanded to 45 degrees.
- After 50s the aircraft is commanded to fly 100m North.
- After 70s, while still flying north, the vehicle is commanded to climb by 20m to its final waypoint.

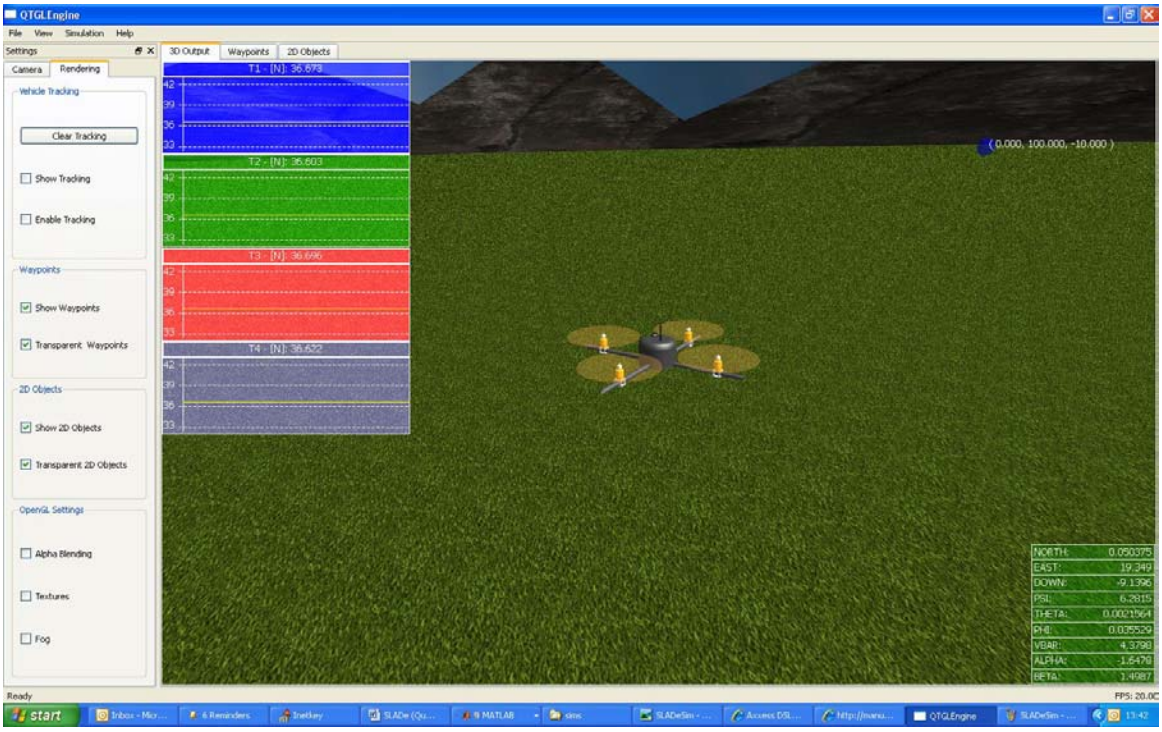

Figure 2 – 3D Graphics Display

The results of the simulation run are shown in Figures 3 and 4. This run shows the ideal case, where the sensors have no noise and there is no wind. It is clear that the aircraft is capable of autonomously tracking the reference trajectory at an arbitrary heading angle. The velocity and position plots (in all three axes) show nicely how the aircraft enters a constant slew rate mode for large reference inputs. Figure 5 shows that reasonable control signals are used to guide the aircraft along the trajectory.

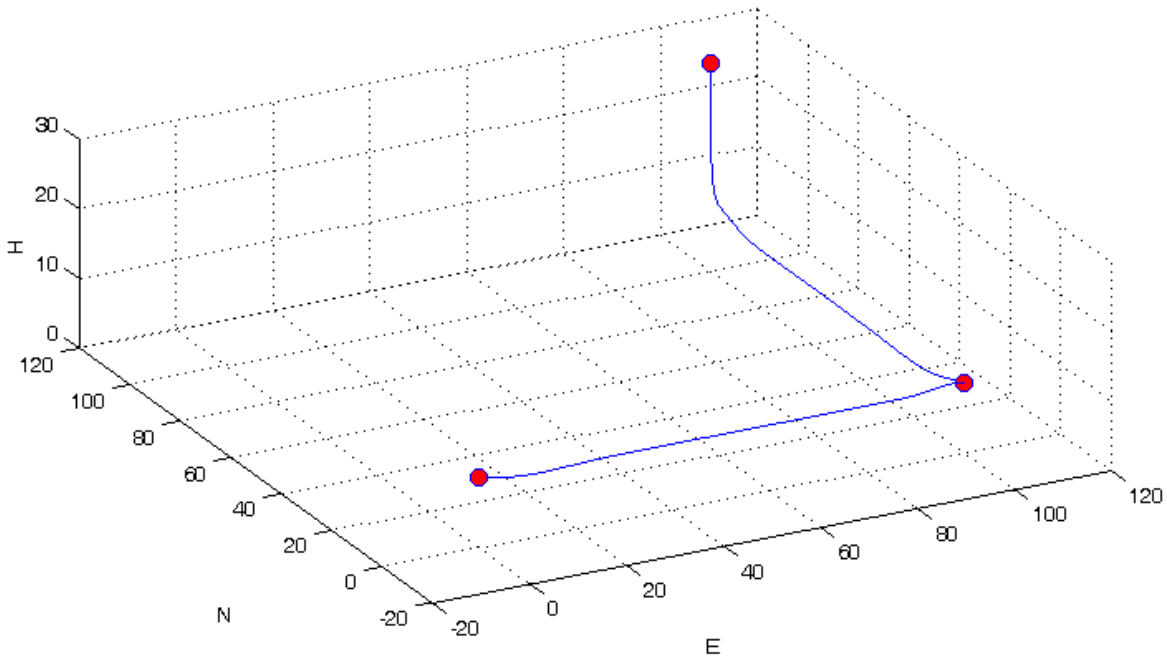

Figure 3 – 3D plot over trajectory

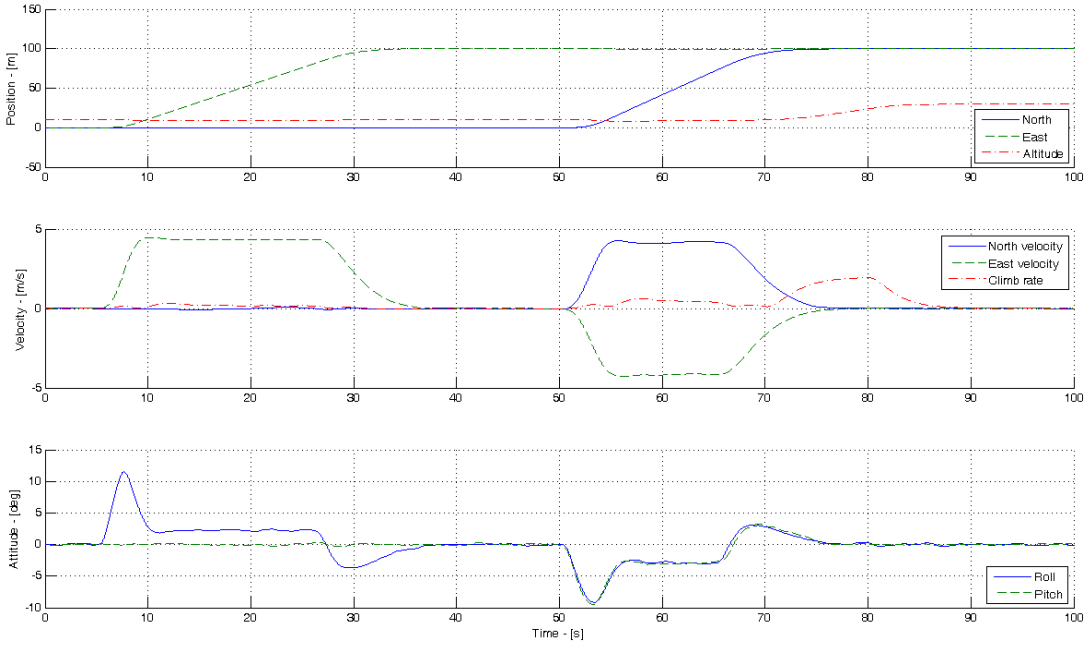

Figure 4 – Simulation results: position, velocity and attitude

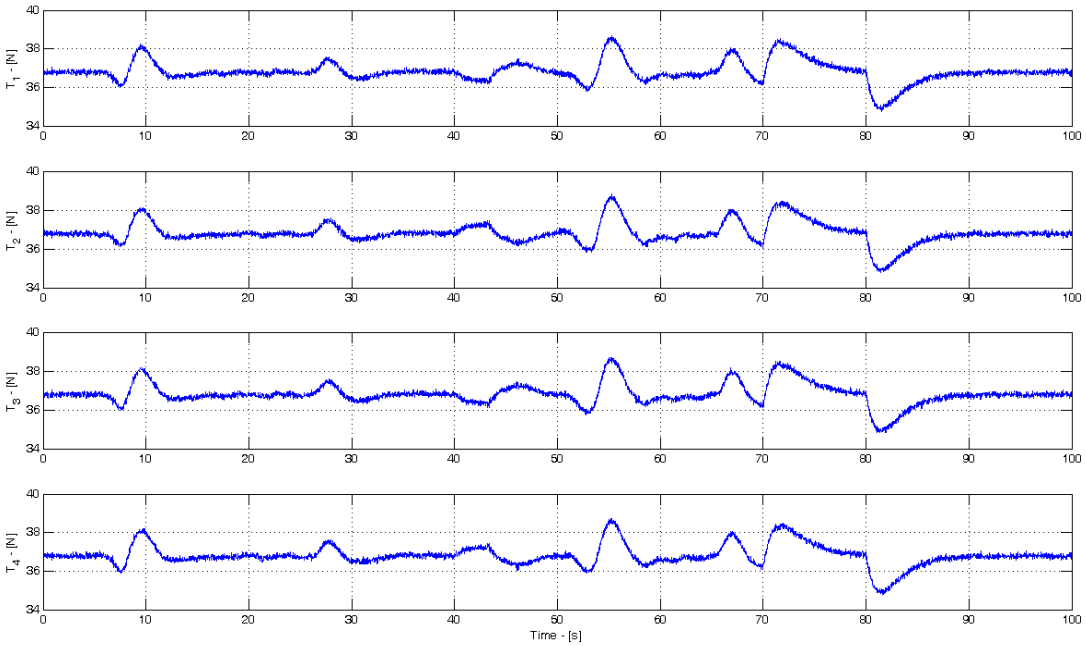

Figure 5 – Actuator commands

Appendix A – SLADe Data

Consider the schematic diagram of the SLADe aircraft below. The orientation of the body axis system with respect to the vehicle is shown. The origin is located at the vehicle's centre of mass, with the $\boldsymbol{k}^{\boldsymbol{B}}$ axis running along the vehicle's geometric centerline in the direction of the airflow. The $\boldsymbol{i}^{\boldsymbol{B}}$ axis points in a predefined forward direction and the $\boldsymbol{j}^{\boldsymbol{B}}$ axis completes the orthogonal, right handed axis system. The rotor thrusts are also labeled T_1 to T_4 respectively. The symbols d and r_D are the roll/pitch torque arm and yaw torque arm to each motor respectively.

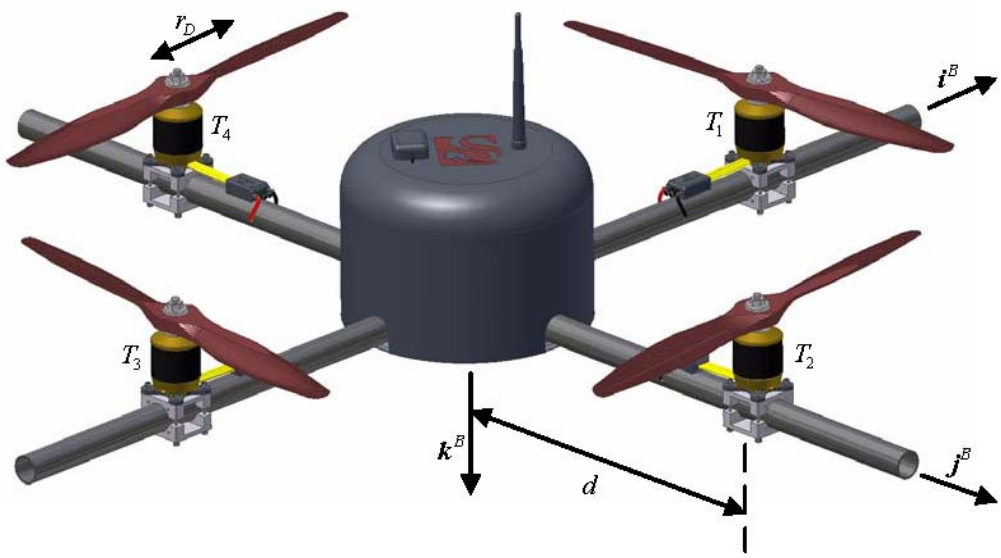

Figure 6 – Schematic of SLADe

SLADe has the following geometric, inertial and aerodynamic properties,

Table 1: Numerical values of symbols for SLADe

Symbol	Value	Unit	Symbol	Value	Unit
d	0.465	m	I_x	0.5	kg m^2
r_D	0.18	m	I_y	0.5	kg m^2
m	15.0	kg	I_z	0.85	kg m^2
A_D	0.5	m^2	C_D	1.0	ND
τ	0.125	s			

where, A_D and C_D are the reference area and coefficient of drag for the entire vehicle respectively.

Appendix B – Feedback Gains

This section lists the feedback gains used for the SLADe aircraft described in Appendix A. All feedback gains were obtained by iterative root locus design, taking into account physical limitations such as actuator saturation.

Longitudinal: $K_{q_P} = 4.0$
$K_{q_I} = 0.8$
$K_\theta = 1.2$
$K_u = -0.06$

Lateral: $K_{p_P} = 4.0$
$K_{p_I} = 0.8$
$K_\phi = 1.2$
$K_v = 0.06$

Directional: $K_{r_P} = 20.0$
$K_{r_I} = 4.0$
$K_\Psi = 0.4$

Heave: $K_{w_P} = -20.0$
$K_{w_I} = -2.0$
$K_D = 0.3$

Navigation: $K_N = 0.25$
$K_E = 0.25$

References

[1] John H. Blakelock, "Automatic Control of Aircraft and Missiles, Second Edition", John Wiley and Sons, 1991.
[2] Willem J. Hough, "Autonomous Aerobatic Flight of a Fixed Wing Unmanned Aerial Vehicle", MSc.Eng Thesis, Stellenbosch University, 2007.
[3] I.K. Peddle, "SLADe – Technical Development Report", 31 July 2007.